

Computational comparison of conductivity and mobility models for silicon nanowire devices

M. Frey,^{1,a)} A. Esposito,¹ and A. Schenk¹

Integrated Systems Laboratory, ETH Zurich, Gloriastr. 35, 8092 Zurich, Switzerland

(Received 25 November 2010; accepted 27 February 2011; published online 20 April 2011)

In this paper, a comparison of three different models for the conductivity and mobility is given for the case of silicon nanowire devices in the presence of electron-phonon scattering. The consistency of all three models in the case of homogeneous nanowires is demonstrated. The scattering limited conductivity and mobility is a well defined quantity in this case. For nonhomogeneous systems like triple-gate nanowires FETs, these scattering limited quantities are no longer well defined for very short gate lengths. The quality of the underlying assumptions and the physical interpretation of the differences in the resulting transport characteristics are discussed. © 2011 American Institute of Physics. [doi:10.1063/1.3573487]

I. INTRODUCTION

The physical properties of the electron inversion layer define the transport characteristics of devices like nanowire FETs (NWFET). With the reduction of both the cross section and the gate length down to nanometer scale, the conductivity and mobility eventually show quite different behavior when compared to devices with a characteristic length scales of tenth of microns. This is due to the nonhomogeneity of the inversion layer and the appearance of quantum mechanical effects like tunneling. The scaling behavior of the conductivity and the mobility as a function of the gate length has been investigated in numerous experimental¹⁻⁵ and simulational studies.⁶⁻⁹ One difficulty lies in the extraction of the mobility from measurements of short-channel FET's: Since different measurement techniques can be applied, a comparison of the data from different publications is not straightforward. A second difficulty is the assumption of different functional dependencies of the current on the mobility and geometrical quantities such as the (effective) gate length in the different publications. Therefore the question arises, whether these different models for the conductivity and mobility can yield identical results. It is the goal of this paper to give a computational comparison of three different models, which are defined in Sec. II B, and discuss the underlying assumptions and the physical interpretation of the differences in the resulting transport characteristics. To study the transport properties of silicon nanowires in the presence of electron-phonon scattering, the nonequilibrium Green's functions formalism^{10,11} (NEGF) is employed. The quantum transport equations are given in Sec. II A. In Sec. II B the different models for the calculation of the conductivity and mobility are presented, which are then applied to two different systems: a homogeneous nanowire in Sec. III A and a triple-gate nanowire FET (TG-NWFET) in Sec. III B and Sec. III C.

II. THEORY

A. Quantum transport equations

Assuming a parabolic band structure for silicon, we express the effective mass Hamiltonian $H(r)$ in the so-called coupled mode expansion.^{12,13} The transport direction x coincides with crystal direction $\langle 100 \rangle$. The steady-state Dyson and Keldysh equation^{14,15} for nanowire devices then read as

$$\sum_{j,m} [E\delta_{ij}\delta_{nm} - H_{ij}(x_n) - \Sigma_{ij}^R(x_n, x_m, E)] \times G_{jk}^R(x_m, x_{n'}, E) = \delta_{ik}\delta_{nn'}, \quad (1)$$

and

$$G_{ij}^<(x_n, x_{n'}, E) = \sum_{k,l,m,m'} [G_{ik}^R(x_n, x_m, E) \times \Sigma_{kl}^<(x_m, x_{m'}, E) G_{lj}^A(x_{m'}, x_{n'}, E)], \quad (2)$$

where G^R and $G^<$ are the solution variables and ij are the mode indices. Carrier-carrier interaction is included in the Hamiltonian via the Hartree potential. The retarded self-energy Σ^R contains the electron-phonon interaction in the device as well as the boundary conditions:

$$\Sigma^R(x_n, x_m) = \Sigma_{\text{scat}}^R(x_n, x_m) + \Sigma_{\text{bc}}^R(x_n, x_m). \quad (3)$$

The electron-phonon scattering is approximated as being local in space;⁷

$$\begin{aligned} \Sigma_{i,j}^<(x_n, x_m, E) &= \sum_{k,l} C_{i,j,k,l}^\pm G_{k,l}^<(x_n, x_m, E \pm \hbar\omega) \delta_{n,m} \\ \Sigma_{i,j}^R(x_n, x_m, E) &= \frac{1}{2} [\Sigma_{i,j}^>(x_n, x_m, E) - \Sigma_{i,j}^<(x_n, x_m, E)] \\ &+ iP \int \frac{dE'}{2\pi} \frac{\Sigma_{i,j}^>(x_n, x_m, E') \Sigma_{i,j}^<(x_n, x_m, E')}{E - E'}, \quad (4) \end{aligned}$$

where $P \int dE'$ is the principal part of the integration which is not neglected in our calculation.¹⁶ The scattering parameters are the same as in Refs. 7 and 17. The Green's functions,

^{a)}Electronic mail: mfrey@iis.ee.ethz.ch.

self-energies and electrostatic potential are iterated until self-consistency is achieved.

B. Definition of conductivity and mobility

1. Kubo–Greenwood formula

Using linear response theory, the conductivity for an open system with a continuous spectrum can be extracted from equilibrium simulations by means of the Kubo–Greenwood formula:^{18–20}

$$\sigma = \sum_v \sum_{i,j} \frac{2\pi e^2 \hbar}{V} \int dE \frac{\partial f(E)}{\partial \mu} \delta(E - H_v) \cdot \delta(E - H_v) v_{ij,v}(E) v_{ji,v}(E), \quad (5)$$

where the sum is taken overall valleys v and modes i, j , and $v_{ij,v}$ is the associated velocity. In terms of Green's functions, this can be rewritten as:^{21–23}

$$\sigma = \sum_v \frac{2\pi e^2 \hbar}{(m_v^*)^2 V} \int dE \frac{\partial f(E)}{\partial \mu} \frac{1}{4\pi^2} \cdot \text{Tr}[\hat{p} A_v(E) \hat{p} A_v(E)], \quad (6)$$

where \hat{p} is the momentum operator and the spectral density function is defined as:

$$A_v(E) = i[G_v^R(E) - G_v^A(E)]. \quad (7)$$

Introducing coordinates leads to:²¹

$$\sigma = \sum_v \frac{-2\pi e^2 \hbar^3}{(m_v^*)^2 V} \int dE \frac{\partial f(E)}{\partial \mu} \frac{1}{4\pi^2} \int_{-\infty}^{\infty} dx_1 \int_{-\infty}^{\infty} dx_2 \times \text{Tr}[\nabla_{x_1} A_v(x_1, x_2, E) \nabla_{x_3} A_v(x_3, x_4, E)|_{x_3=x_2}^{x_4=x_1}]. \quad (8)$$

For a homogeneous system, it can be shown²³ that the leading term of Eq. (8) has the form:^{20,23}

$$\sigma(x_n) = \sum_v \sum_i \frac{e^2}{V(x_n)} \int dE \left[\frac{\tau_{i,v}(x_n, E)}{m_v^*} \frac{[\hbar \text{Re}(k_i)]^2}{2m_v^*} \cdot A_{ii,v}(x_n, x_n, E) \frac{\partial f(E)}{\partial \mu} \right], \quad (9)$$

as expected from semiclassical transport theory, i.e., from the Boltzmann equation. The individual quantities in Eq. (9) are defined as follows:

$$\tau_{i,v}(x_n, E) := \hbar \left[\text{Im} \left[\sum_{ii,v}^{R, \text{scat}}(x_n, x_n, E) \right] \right]^{-1}, \quad (10)$$

$$k_i := k_{i,v}(x_n, E) = \frac{\sqrt{2m_v^* [E - E_{i,v}(x_n) - \sum_{ii,v}^{R, \text{scat}}(x_n, x_n, E)]}}{\hbar}, \quad (11)$$

and $V(x_n)$ is the volume of the slice associated with x_n .

From the definition of the conductivity, the mobility $\mu(x_n)$ can be written as:^{7,24}

$$\begin{aligned} \mu(x_n) &= \frac{1}{n(x_n)} \sum_v \sum_i \mu_{i,v}(x_n) n_{i,v}(x_n), \\ &= \frac{1}{en(x_n)} \sum_v \sum_i \sigma_{i,v}(x_n), \\ &= \frac{\sigma(x_n)}{en(x_n)}. \end{aligned} \quad (12)$$

It is obvious, that in the case of a homogeneous system, the local conductivity and mobility in Eq. (9) and Eq. (12) must be constant throughout the device.

2. Macroscopic definition

The resistivity of a rectangular device, which in general is an inhomogeneous system, is given by the partial derivative of the resistance

$$R(L) = \frac{V_{DS}}{I_D(L)}, \quad (13)$$

with respect to the device length L :

$$\rho(L) := \frac{\partial R(L)}{\partial L} \cdot A_{\text{cross}}, \quad (14)$$

where V_{DS} is the applied bias, $I_D(L)$ the total current and A_{cross} is the uniform cross section of the device. The conductivity is then defined as the inverse of the resistivity:

$$\sigma(L) := [\rho(L)]^{-1} = \left(\frac{\partial R(L)}{\partial L} \right)^{-1} \cdot \frac{1}{A_{\text{cross}}}. \quad (15)$$

In this case, the conductivity and mobility are determined from a nonequilibrium simulation. The mobility is obtained by inserting Eq. (15) into Eq. (12).

3. Shur model

Following the concept of the simple Drude model, an effective conductivity or mobility can be defined, to which the current I_D is proportional:

$$I_D \propto \sigma_{\text{eff}} \Leftrightarrow R \propto (\sigma_{\text{eff}})^{-1}. \quad (16)$$

However, in devices such as nanowires, there are several contributions to the resistance and these individual contributions show different scaling behavior with respect to the device geometry. Therefore, a distinction was introduced between the contributions that can be associated with a well-defined scattering mechanism, as for example electron-phonon scattering, while all other contributions are lumped into a single term.^{8,25} The first type of contributions is labeled scattering limited conductivity σ_{scat} while the latter gives rise to the so-called ballistic conductivity σ_{bal} . The different conductivities are related by assuming Matthiessen's rule to be valid:

$$\frac{1}{\sigma_{\text{eff}}(L)} := \frac{1}{\sigma_{\text{scat}}(L)} + \frac{1}{\sigma_{\text{bal}}(L)}. \quad (17)$$

This is equivalent to demand the additivity of the different resistance contributions:

$$R(L) = R_{\text{scat}}(L) + R_{\text{bal}}(L). \quad (18)$$

Note that in order to determine $\sigma_{\text{scat}}(L)$, two types of nonequilibrium simulations need to be carried out:

- (1) A computation of the total current I_D , including scattering effects, and
- (2) the computation of I_D^{bal} , i.e., a ballistic simulation without scattering effects

The quantity $\sigma_{\text{eff}}(L)$ is calculated in the following way:

$$\sigma_{\text{eff}}(L) := G(L) \frac{L}{A_{\text{cross}}} \approx \frac{I_D(L)}{V_{DS}} \frac{L}{A_{\text{cross}}}. \quad (19)$$

In Eq. (19) the conductance $G(L)$ was approximated with the ratio of the current divided by the applied voltage V_{DS} , which is only valid in the linear response regime, i.e., for a small applied bias. The calculation of $\sigma_{\text{bal}}(L)$ is done by using I_D^{bal} instead of I_D in Eq. (19).

Note that in Shur's definition, the device length L (or the gate length L_G in case of TG-NWFETs) explicitly enters the expressions for the conductivity and the mobility, unlike the definitions in Secs. II B 1 and II B 2.

III. RESULTS

A. Conductivity of resistors

The first category of nanowire based devices used in this study is labeled *Resistors*. The detailed specifications are: A silicon cross-section of $t_{\text{Si}} \times t_{\text{Si}} = 3 \times 3 \text{ nm}^2$, a silicon dioxide layer of thickness $t_{\text{ox}} = 0.6 \text{ nm}$ wrapped all around the silicon, device lengths between $L = 10 \text{ nm}$ and $L = 60 \text{ nm}$ with a homogeneous arsenic doping concentration of $N_D = 2e20 \text{ cm}^{-3}$.

In the equilibrium state of a resistor with Ohmic contacts, the electrostatic potential and therefore all subbands must be constant along the transport direction x in the device. This cannot be achieved by the standard boundary conditions for the quantum transport equations, where scattering in the contacts is ignored, resulting in the injection of coherent states from the contacts into the device.²⁶ Therefore, scattering in the contacts must be taken into account, resulting in incoherent injection.^{27,28} In the case of local electron-phonon scattering, the equilibrium state of the (infinite) homogeneous system can be computed in an exact way, since the analytical form of the Green's functions are known. A detailed description of the boundary conditions used in this work can be found in the references.^{27,29}

In order to be able to compare the conductivities obtained from the three different models described in Sec. II B, a restriction to the linear response regime is necessary. In Fig. 1 the current is shown as function of a small applied bias $eV_{DS} < k_B T$, for several device lengths. In Fig. 2 the scaling behavior of the resistance

$$R(L) := \frac{V_{DS}}{I_D(L)}, \quad (20)$$

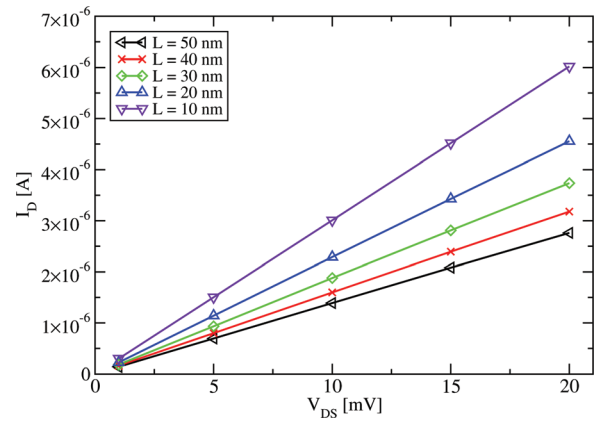


FIG. 1. (Color online) The current is a linear function of the small applied bias.

as a function of the device length L is shown. As expected, all curves collapse to a single straight line, i.e., the resistance is of the form:

$$R(L) = R_{\text{scat}}(L) + R_{\text{bal}} = \rho \frac{L}{A_{\text{cross}}} + (G_{\text{bal}})^{-1}, \quad (21)$$

where $\rho \neq \rho(L)$ and $R_{\text{bal}} \neq R_{\text{bal}}(L)$ are constants, solely defined by the cross section and the material. Note that R_{bal} in Eq. (21) must be computed from an equilibrium simulation, since self-consistent nonequilibrium simulations within the ballistic transport regime do not converge for resistors, due to the lack of an internal resistance.²⁹ Instead the Landauer-Büttiker formalism is used to compute G_{bal} from an equilibrium simulation.³⁰

$$G_{\text{bal}} = 10.2 \frac{e^2}{h} \rightarrow R_{\text{bal}} = 2.5 \text{ k}\Omega. \quad (22)$$

Despite this drawback, it is clear from the results in Fig. 2 that the quantity σ_{scat} in Eq. (17) is still well defined in the case of resistors and can be calculated with the help of Eq. (19) and Eq. (21). No such difficulties occur if the definition (15) is applied. The derivative of the resistance with respect to the device length is evaluated on a linear fit of the data, as shown in Fig. 2:

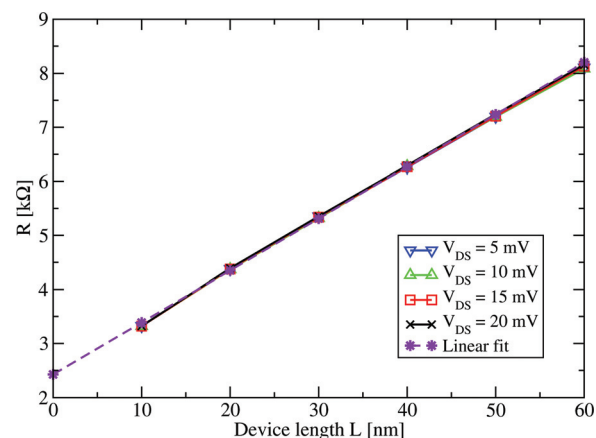


FIG. 2. (Color online) For the Resistors, all resistance curves obtained for the different applied voltages collapse to a single straight line, resulting in Ohmic scaling behavior.

TABLE I. A summary of the calculated conductivities from the different definitions. The variance of the conductivity calculations $\Delta\sigma$ is also shown. In the case of the Resistors they all coincide and yield the scattering limited conductivity σ_{scat} .

Definition	Eq. (8)	Eq. (9)	Eq. (15)	Eq. (17)	
σ	0.831	0.816	0.806	0.802	$e^2(ha_0)^{-1}$
$\Delta\sigma$	0.010	0.011	0.015	0.015	$e^2(ha_0)^{-1}$

$$\frac{\partial R(L)}{\partial L} = 96 \pm 2 \frac{\Omega}{\text{nm}} \rightarrow \sigma = 0.806 \pm 0.015 \frac{e^2}{ha_0}. \quad (23)$$

Extrapolating the linear fit toward $L \rightarrow 0$ yields the inverse of the ballistic equilibrium conductance G_{bal} . It is straightforward to see from Eqs. (15) and (21), that the macroscopic definition of the conductivity results in the scattering limited conductivity σ_{scat} of Eq. (17). As the last step, the conductivity is computed by means of the Kubo–Greenwood formulas (8) and (9). The summary of all results is given in Table I.

From the discussion above we conclude, that all definitions yield the scattering limited conductivity σ_{scat} in the case of Resistors.

B. Conductivity of triple-gate nanowire FETs

The second category of devices are TG-NWFETs. The detailed specifications are: A silicon cross-section of $t_{\text{Si}} \times t_{\text{Si}} = 5 \times 5 \text{ nm}^2$, a silicon dioxide layer of thickness $t_{\text{ox}} = 0.6 \text{ nm}$ wrapped all around the silicon, and various gate lengths from $L_G = 3 \text{ nm}$ up to $L_G = 40 \text{ nm}$. In all simulated TG-NWFETs the source and drain extension are 10 nm long and homogeneously doped with an arsenic doping concentration of $N_D = 2e20 \text{ cm}^{-3}$, while the channel remains undoped.

As in the case of the resistors in Sec. III A, a restriction to the linear response regime is necessary in order to allow a comparison of the different conductivity definitions. In the following, a source-drain bias of $V_{DS} = 5 \text{ mV}$ is used for all nonequilibrium simulations. The scaling of the resistance $R(L_G)$ as a function of the gate length L_G for different gate voltages V_{GS} is shown in Fig. 3. In the limit $L_G \rightarrow 0$ the TG-NWFET becomes a resistor of device length $L = 2 \times 10 \text{ nm} = 20 \text{ nm}$. Therefore all curves for the different gate voltages V_{GS} merge at $L_G = 0 \text{ nm}$. The scaling behavior of

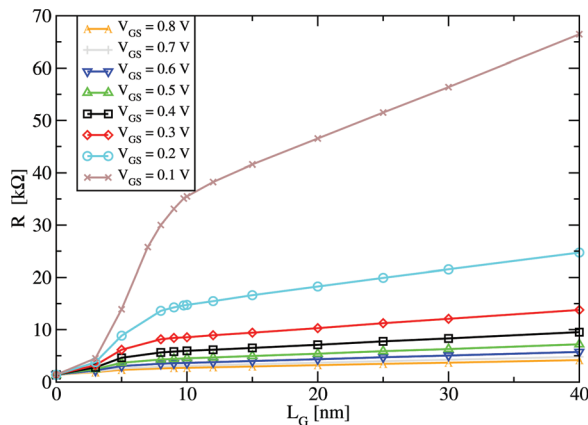


FIG. 3. (Color online) The resistance of TG-NWFETs as a function of the gate length and the gate voltage. The source-drain bias is $V_{DS} = 5 \text{ mV}$.

the resistance in the interval $L_G = 0 \rightarrow 10 \text{ nm}$ is dominated by the tunneling component of the current. Obviously the change in the resistance is larger for smaller gate voltages, i.e., when the source-to-drain barrier is higher. For larger gate lengths $10 \text{ nm} < L_G < 20 \text{ nm}$, the transition between the ballistic regime and the Ohmic regime occurs. It is worthwhile to note, that the ballistic resistance does depend on the gate length L_G , but not on the length of the source-drain extension, while the resistance associated with electron-phonon scattering depends on both. This is true for the case of quantum transport as well as for semiclassical transport models based on the Boltzmann equation.^{6,31}

In order to compute the conductivity from the macroscopic definition Eq. (15), the derivative is evaluated on a fit $F[R(L_G)]$ of the data in Fig. 3, which is of the form

$$F[R(L_G)] = a \cdot \left(1 + e^{-b(L_G-c)}\right)^{-1} + d \cdot L_G + e, \quad (24)$$

having five degrees of freedom a, b, c, d, e . For the computation of σ_{eff} and σ_{bal} for TG-NWFETs using Shur's definition, the device length L must be replaced by the gate length L_G in Eq. (19).^{9,32} Then σ_{scat} can be calculated from Eq. (17). Unlike a resistor, a TG-NWFET is an inhomogeneous system. Thus, strictly speaking, the Kubo–Greenwood formula (9) is no longer valid. However it is plausible, that in the limit of a vanishing bias $V_{DS} \rightarrow 0$ and long gate lengths $L_G \gg \lambda_T$ and $L_G \gg \lambda_{\text{mfp}}$, where λ_T is the DeBroglie wave length and λ_{mfp} is the mean free path, the inversion layer under the gate contact is a quasihomogeneous system, determining the conductivity of the device. In the regime $L_G > \lambda_T$, where tunneling and other coherent effects begin to occur, this is no longer the case. To study the validity and the breakdown of the Kubo–Greenwood formula, the respective conductivities were evaluated in the middle of the gate. This is in contrast to the macroscopic definition, where the influence of the entire device is automatically included, without any ambiguity. In Shur's definition, the influence of the entire device enters through the current, yet two types of simulations are required and an additional functional dependence of the conductivity on the gate length is assumed. As already mentioned, it also requires the validity of

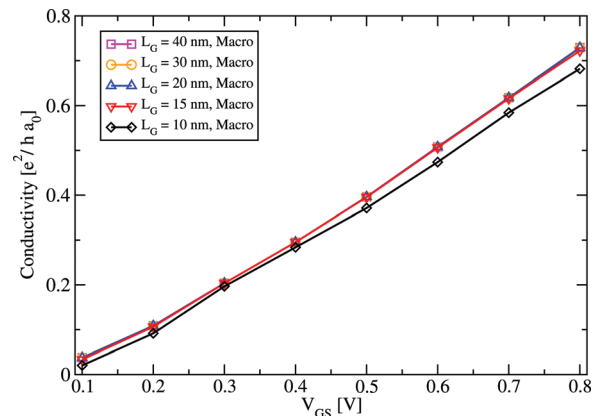


FIG. 4. (Color online) The conductivities of TG-NWFETs computed with the macroscopic definition (macro) of Eq. (15), using the fit formula given in Eq. (24).

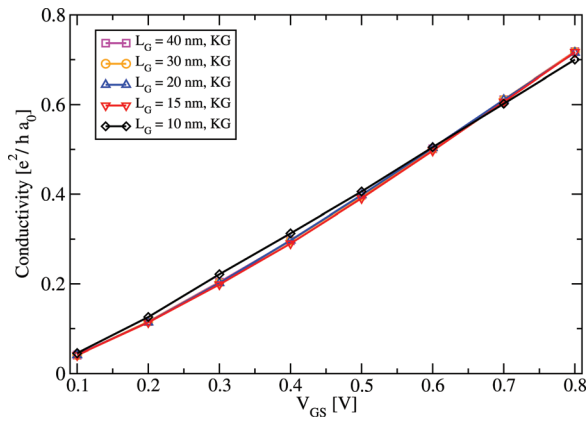


FIG. 5. (Color online) The conductivities of TG-NWFETs computed with the Kubo–Greenwood formula (KG) of Eq. (9), which was evaluated in the middle of the channel: $x_n = 0.5 \cdot L$.

Matthiessen’s rule. The results of the three definitions are shown in Figs. 4–6. The relative differences are shown in Fig. 7, where the results from the Kubo–Greenwood formula and Shur’s model are compared to the macroscopic definition:

$$\sum_{V_{GS}} \frac{|\sigma_{KG}(L_G, V_{GS}) - \sigma_{Macro}(L_G, V_{GS})|}{\sigma_{Macro}(L_G, V_{GS})}, \quad (25)$$

and

$$\sum_{V_{GS}} \frac{|\sigma_{shur}(L_G, V_{GS}) - \sigma_{Macro}(L_G, V_{GS})|}{\sigma_{Macro}(L_G, V_{GS})}. \quad (26)$$

For gate lengths $L_G \geq 20$ nm, the macroscopic and the Kubo–Greenwood model are identical up to a numerical error of 3%. For $L_G \approx 15$ nm, which is in the transition region between the ballistic and the Ohmic regime, this difference increases up to 5–6%, and increases further as the gate length decreases, due to the breakdown of the assumptions for the Kubo–Greenwood model, i.e., the required quasi-homogeneity of the system.

Next we discuss the comparison of Shur’s model to the macroscopic definition. The reason for the drastic relative difference of 50% for $L_G = 10$ nm lies in the fact, that the macroscopic definition automatically takes tunneling effects into

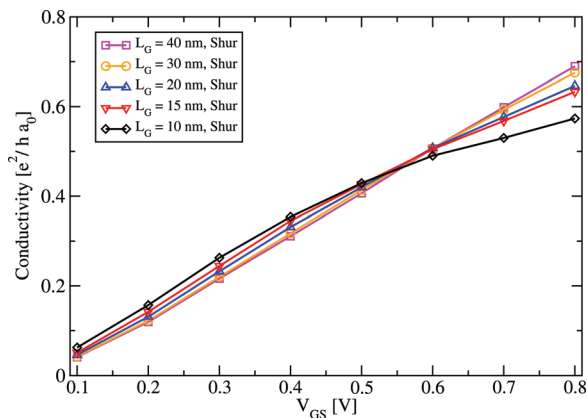


FIG. 6. (Color online) The conductivities σ_{scat} of TG-NWFETs computed with Shur’s definition (Shur) in Eq. (17).

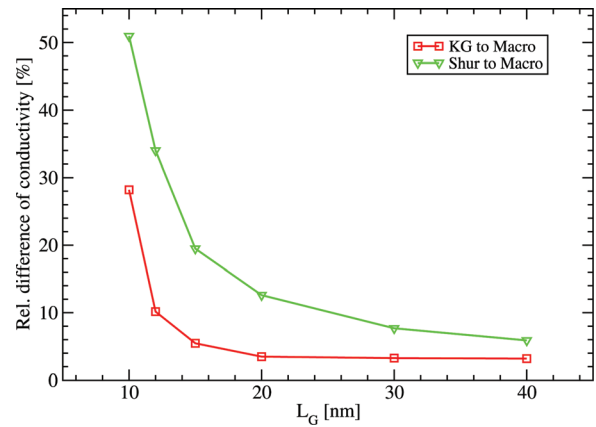


FIG. 7. (Color online) The relative differences of the conductivities as defined in Eqs. (25) and (26).

account, i.e., it can no longer be identified with σ_{scat} from the Shur definition as in the case of the resistors. These tunneling effects are dominant for short gate lengths and low gate voltages. Although the relative difference between Shur’s model and the macroscopic definition does decrease for increasing gate lengths, it is still larger than 6% even for $L_G = 40$ nm. This is either due to a higher numerical error of Shur’s method or a violation of an underlying assumption. A small numerical error in σ_{eff} and σ_{bal} can lead to a relatively large error in

$$\sigma_{scat}(L_G) = \frac{\sigma_{eff}(L_G) \cdot \sigma_{bal}(L_G)}{\sigma_{bal}(L_G) - \sigma_{eff}(L_G)}, \quad (27)$$

especially if current is dominated by ballistic effects, e.g., $\sigma_{eff} \approx \sigma_{bal}$. On the other hand, a certain part of the ballistic resistance $R_{bal} = V_{DS} \cdot (I_D^{bal})^{-1}$ is due to tunneling currents. The assumption that such kind of resistance obeys Matthiessen’s rule is rather fallacious.

In the end, it is clear from Fig. 7 and the underlying equations that for large gate lengths $L_G > 40$ nm, all three definitions of the conductivity eventually yield the same result.

C. Mobility of triple-gate nanowire FETs

Using the definition in Eq. (12), the mobility can be computed for the three different models, as shown in Figs. 8–10.

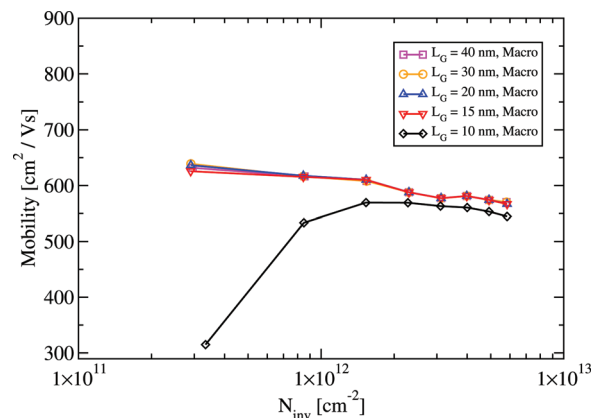


FIG. 8. (Color online) The mobility computed with the macroscopic definition (macro) of Eqs. (15) and (12). N_{inv} was evaluated in the middle of the channel: $x_n = 0.5 \cdot L$.

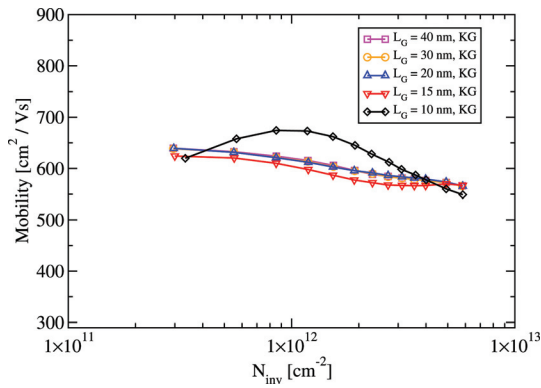


FIG. 9. (Color online) The mobility computed with the Kubo–Greenwood formula (KG) in Eqs. (9) and (12). N_{inv} was evaluated in the middle of the channel: $x_n = 0.5 \cdot L$.

The inversion-charge density N_{inv} was evaluated in the middle of the channel. While N_{inv} is almost constant for gate lengths $L_G > 15$ nm (and a fixed gate voltage), its value increases for shorter gate lengths due to tunneling, resulting in a reduction of the mobility. This effect is more pronounced in the case of high source-to-drain barriers, i.e., for the lower gate voltages. Comparing the results of Fig. 8 to Fig. 9, we find a good agreement between the macroscopic and the Kubo–Greenwood data for all gate lengths $L_G \geq 15$ nm. This is trivial given the results for the conductivity of the two models in Sec. III B. On the other hand, the mobility data computed with Shur’s model shows quite different characteristics for the gate lengths $L_G \leq 20$ nm. While the saturation mobility for the smaller gate lengths increases for low values of N_{inv} , the decrease of the mobility in Fig. 10 is stronger with increasing N_{inv} than in Fig. 8 and Fig. 9.

IV. CONCLUSION

The question of the proper definition for the scattering limited conductivity and mobility have been discussed for quantum transport in silicon nanowires in the presence of electron-phonon scattering. In the case of homogeneous systems as resistors, it was shown that all three models discussed here coincide and yield the scattering limited conductivity, which is a well defined quantity for such systems. For nonhomogeneous systems as TG-NWFETs, this is in general no longer the case, since there are different contributions to the resistance with a completely different scaling behavior. While the results for both conductivity and mobility from the macroscopic model and the Kubo–Greenwood formula match down to gate lengths of $L_G = 15$ nm with a relative difference of less than 6%, the results from Shur’s definition deviate much stronger. For a very short gate length $L_G = 10$ nm, the results of the models are in complete disagreement. For long gate lengths $L_G \geq 40$ nm, when quasihomogeneity of the system is recovered, all results converge and the scattering limited conductivity is well defined again.

ACKNOWLEDGMENTS

The authors would like to thank D. Oehri for interesting discussion and hints. This work had financial support from EU-IST-216171(NANOSIL).

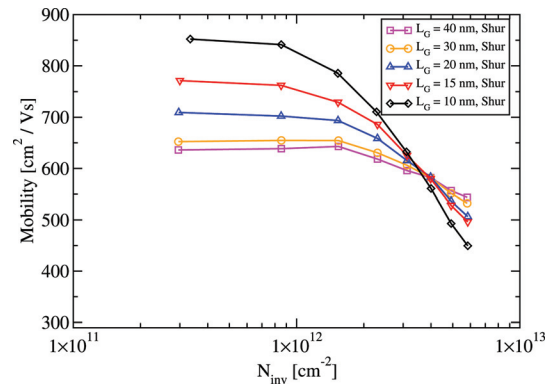


FIG. 10. (Color online) The mobility computed with Shur’s definition of Eqs. (17) and (12). N_{inv} was evaluated in the middle of the channel: $x_n = 0.5 \cdot L$.

- ¹A. Cros, K. Romanjek, D. Fleury, S. Harrison, R. Cerutti, P. Coronel, B. Dumont, A. Pouydebasque, R. Wacquez, B. Duriez, R. Gwoziecki, F. Boeuf, H. Brut, G. Ghibaudo, and T. Skotnicki, “Unexpected mobility degradation for very short devices: A new challenge for CMOS scaling,” in *Electron Devices Meeting, 2006. IEDM’06 International pages 1–4*. (IEEE, New York, 2007), pp. 1–4.
- ²Y. M. Meziani, J. Łusakowski, W. Knap, N. Dyakonova, F. Teppe, K. Romanjek, M. Ferrier, R. Clerc, G. Ghibaudo, F. Boeuf, T. Skotnicki, D. Maude, S. Romyantsev, and M. S. Shur, *J. Appl. Phys.* **96**, 5761 (2004).
- ³S. Severi, L. Pantisano, E. Augendre, E. San Andres, P. Eyben, and K. De Meyer, *IEEE Trans. Electron Devices* **54**, 2690 (2007).
- ⁴Y. Taur, *IEEE Trans. Electron Devices* **47**, 160 (2002).
- ⁵R. Wang, H. Liu, R. Huang, J. Zhuge, L. Zhang, D. W. Kim, X. Zhang, D. Park, and Y. Wang, *IEEE Trans. Electron Devices* **55**, 2960 (2008).
- ⁶E. Gnani, A. Gnudi, S. Reggiani, and G. Baccarani, *IEEE Trans. Electron Devices* **57**, 336 (2010).
- ⁷S. Jin, Y. J. Park, and H. S. Min, *J. Appl. Phys.* **99**, 123719 (2006).
- ⁸A. A. Kastalsky and M. S. Shur, *Solid State Commun.* **39**, 715 (1981).
- ⁹S. Poli and M. G. Pala, *IEEE Electron Device Lett.* **30**, 1212 (2009).
- ¹⁰A. A. Abrikosov and L. P. Gorkov, *Methods of Quantum Field Theory in Statistical Physics* (Dover, New York 1975).
- ¹¹L. P. Kadanoff and G. Baym, *Quantum Statistical Physics* (Benjamin, New York 1962).
- ¹²M. Luisier, A. Schenk, and W. Fichtner, *J. Appl. Phys.* **100**, 043713 (2006).
- ¹³R. Venugopal, Z. Ren, S. Datta, M. S. Lundstrom, and D. Jovanovic, *J. Appl. Phys.* **92**, 3730 (2002).
- ¹⁴F. J. Dyson, *Phys. Rev.* **75**, 486 (1949).
- ¹⁵L. V. Keldysh, *Zh. Eksp. Teor. Fiz.* **47**, 151 (1964).
- ¹⁶A. Esposito, M. Frey, and A. Schenk, *J. Comput. Electron.* **8**, 336 (2009).
- ¹⁷C. Jacoboni and L. Reggiani, *Rev. Mod. Phys.* **55**, 645 (1983).
- ¹⁸D. A. Greenwood, *Proc. Phys. Soc.* **71**, 585 (1958).
- ¹⁹R. Kubo, *J. Phys. Soc. Jpn.* **12**, 570 (1957).
- ²⁰G. D. Mahan, *Many-Particle Physics* (Plenum, New York, 1990).
- ²¹S. F. Edwards, *Philos. Mag.* **3**, 1020 (1958).
- ²²J. Rubio, *J. Phys. C: Solid State Phys.* **2**, 288 (1969).
- ²³B. Velicky, *Phys. Rev.* **184**, 614 (1969).
- ²⁴H. Jiang, S. Shao, W. Cai, and P. Zhang, *J. Comput. Phys.* **227**, 6553 (2008).
- ²⁵M. S. Shur, *IEEE Electron. Device Lett.* **23**, 511 (2002).
- ²⁶R. C. Bowen, W. R. Frensley, G. Klimeck, and R. K. Lake, *Phys. Rev. B* **52**, 2754 (1995).
- ²⁷M. Frey, A. Esposito, and A. Schenk, *Proc. IWCE* **13**, 17 (2009).
- ²⁸M. J. McLennan, Y. Lee, and S. Datta, *Phys. Rev. B* **43**, 13846 (1991).
- ²⁹M. Frey, “Scattering in Nanoscale Devices,” Ph.D. dissertation, ETH Zurich, 2010.
- ³⁰M. Büttiker, Y. Imry, R. Landauer, and S. Pinhas, *Phys. Rev. B* **31**, 6207 (1985).
- ³¹E. Gnani, A. Gnudi, S. Reggiani, and G. Baccarani, *IEEE Trans. Electron Devices* **55**, 2918, 2008.
- ³²S. Poli, “Modelling and Simulations of POST-CMOS Devices,” Ph.D. dissertation, University of Bologna, 2009.